2013 10th IEEE International Conference on Control and Automation (ICCA)
Hangzhou, China, June 12-14, 2013

Design of Blended Control Strategy for Autonomous Aircrafts with Multiple Actuators *

Zhen Liu, Ruyi Yuan, Guoliang Fan, Jianqiang Yi, *Senior Member, IEEE,* and Hanbo Qian

***Abstract*—A blended control strategy for autonomous aircrafts with multiple actuators is proposed in this paper. The strategy is divided into aerodynamic control subsystem and reaction jet control subsystem (RCS). Due to the complex nonlinearities, large uncertainties and strong coupling, the aerodynamic subsystem controller is designed by applying feedback linearization based on the theory of time-scale separation and sliding mode control theory. The RCS consists of four parts that are error dynamic adjustment model, PD controller, firing logic algorithm and reaction jet model. The RCS, which corresponds with the actual engineering characteristics of attitude control motors (ACMs), is designed to improve the response performance. Simulation results with a nonlinear six-dimension aircraft model show the blended control strategy has a higher tracking precision and a much more improved response characteristic than pure aerodynamic control. Simultaneously the robustness for the aerodynamic coefficient uncertainties and jets interaction is strong.**

Index Terms*— Blended control strategy, multiple actuators, feedback linearization, sliding mode control, firing logic algorithm

I. INTRODUCTION

The future autonomous aircrafts are required to possess further range, faster speed and higher maneuverability. In the respect of maneuverability, most of the present-day autonomous aircrafts employ only aerodynamic fins, and cannot achieve fast time response or high maneuverability, because of the loss of aerodynamic effectiveness when the vehicles are at higher altitudes or lower speeds. So there must be some technologies to compensate this loss. Two common efforts for the problem are thrust vector control (TVC) and reaction jet control system (RCS) [1]-[3]. This paper is concerned with autonomous aircrafts using RCS to improve the speed of response and maneuverability.

The reaction jet control system consists of a certain amount of attitude control motors (ACMs) [5]. These ACMs are solid rocket motors, and can only provide constant and discrete control forces. This is different from the aerodynamic forces generated by the fins which can be continuously changed. Moreover, when the ACMs are fired, it would bring significant influence of interaction between aerodynamic flow and jet plumes [4][6]. These factors necessitate the development of blended control systems which can handle complex nonlinearities, large uncertainties and multiple actuators [7]. Many theoretical efforts about this have been achieved. Some attentions in these researches are focused on the pitch plane [1]-[4], and the control power of RCS is often simplified to be continuous and adjustable [9]-[12]. Yet there are recently some papers which consider the two kinds of totally different actuators. Ref. [6] designed a combined control system, using linear quadratic optimal control theory and a firing logic of ACMs based on superposition algorithm. Ref. [14] presented an aerodynamic control system based on dynamic inversion and active disturbance rejection control, and designed an integer linear programming method to adjust the RCS. Ref. [15] applied hybrid system control theory to achieve reasonable allocation of energy between two modes.

This paper presents a blended control strategy based on dividing the whole attitude control system into two separate parts, which are aerodynamic control subsystem and reaction jet control subsystem. For the complex nonlinearities, large uncertainties and strong coupling, the aerodynamic control subsystem takes the combination of feedback linearization and sliding mode control theory. The feedback linearization is used to linearize and decouple the attitude system of the aircraft, while the sliding mode control acts to guarantee the robustness for uncertainties and disturbance. For the reaction jet control subsystem, a firing logic of the ACMs, which takes the actual engineering characteristics of the RCS into consideration, is designed to improve the response speed. Finally, a nonlinear six-dimension autonomous aircraft, which includes aerodynamic coefficient uncertainties and the influence of interaction between aerodynamic flow and jet plumes, is used to simulate the blended control strategy. The results show the blended control system is satisfied with the requirements of fast-speed, high-accuracy and strong robustness simultaneously.

II. DYNAMIC MODEL

The body model of the autonomous aircraft employed here refers to the PAC-3 missile [5][8] as shown in Fig. 1. It is a very common aerodynamic configuration for anti-air aircrafts. A standard cruciform axial-symmetric shape with fixed wings and all-moved fins is used, and the ACMs are located in front of the aircraft's center of mass. For describing the attitude motion of the autonomous aircraft, the body-fixed frame of reference is needed. As shown in Figure 1, the origin of the body-fixed reference frame is at the aircraft's center of mass, while the X_B -axis points forward in the direction of the aircraft nose, the Y_B -axis in the right starboard direction, and

* Resrach supported by the National Natural Science Foundation of China (No. 61273149, 61203003) and the Special Project for Innovation Methods of MOST (No. 2012IM010200).

Zhen Liu is with the Institute of Automation, Chinese Academy of Sciences, Beijing, China (e-mail: liuzhen@ia.ac.cn).

Ruyi Yuan, Guoliang Fan and Jianqaing Yi are with the Institute of Automation, Chinese Academy of Sciences, Beijing, China (email: ruyi.yuan, guoliang.fan, jianqiang.yi@ia.ac.cn).

Hanbo Qian is with the Center of Coordination & Support of SASTIND, Beijing, China (e-mail: qianhanbo160@163.com).

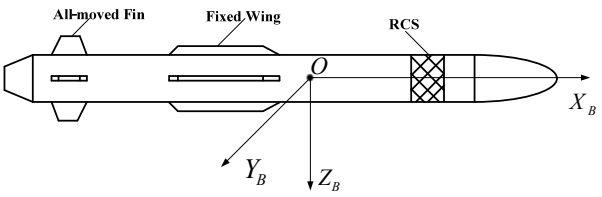

Figure 1. Autonomous aircraft configuration

the Z_B -axis downwards.

A. Autonomous aircraft model

A nonlinear six degrees of freedom aircraft is investigated here. Ref. [8] shows the most commonly used mathematical model for aircraft motion study. Based on these previous efforts, the model with aerodynamic fins and reaction jets is described as

$$\begin{aligned}\dot{\alpha} &= q-(p\cos\alpha + r\sin\alpha)\tan\beta \\ &\quad +(C_z QS + T_z)\cos\alpha/(mV\cos\beta) \\ &\quad -(C_x QS + T_z)\sin\alpha/(mV\cos\beta)\end{aligned} \tag{1}$$

$$\begin{aligned}\dot{\beta} &= -r\cos\alpha + p\cos\alpha \\ &\quad +(C_y QS + T_y)\cos\beta/(mV) \\ &\quad -(C_z QS_z + T_z)\sin\beta\sin\alpha/(mV) \\ &\quad -(C_x QS + T_z)\sin\beta\cos\alpha/(mV)\end{aligned} \tag{2}$$

$$\dot{p} = C_l QSL_{ref}/I_x \tag{3}$$

$$\dot{q} = pr(I_z - I_x)/I_y + (C_m QSL_{ref} - T_z l)/I_y \tag{4}$$

$$\dot{r} = pq(I_x - I_y)/I_z + (C_n QSL_{ref} + T_y l)/I_z \tag{5}$$

where α and β are angle of attack and angle of sideslip respectively; p,q,r are the components of the body rotational rate; Q is the dynamic pressure; L_{ref} is the reference length and S the reference area; l is the distance between the aircraft's center of mass and the fired reaction jets. T_x, T_y, T_z are the lateral thrusts acting along the body axes generated by the reaction jets. The aircraft moments of inertia are denoted by I_x, I_y, I_z . The aerodynamic force and moment coefficients $C_x, C_y, C_z, C_l, C_m, C_n$ are functions with respect to Mach number M , altitude H , α , β and the deflection of the aerodynamic fin δ . These data are usually obtained from wind tunnel test, here yet Datcom code is used to figure out the numerical values at particular points, and then linear interpolation is performed to look for the others.

B. Model of reaction jet system

As described above, the reaction jet control system consists of a certain amount of attitude control motors (ACMs). These ACMs are evenly arranged in rings around the aircraft's body axis and thrust perpendicularly to the body axis to provide pitch and yaw control during the homing phase [5]. The neighboring rings are staggered arrangement. Referring to PAC-3, the number of rings is 10 and there are 18 motors each ring. Each motor is signed (i, j) , where i denotes the serial number of the ring and j the placement in the *ith* ring. The configurations of the ACMs in both odd and even rings are shown in Fig. 2.

As the diameter of the ACMs is very small which can be ignored, a virtual marking method [6] is used to mark the ACMs here. In this method, each odd ring is combined with its neighboring even ring. So the number of virtual rings is reduced to a half, and each virtual ring would have twice motors as shown in Figure 3. Moreover, this will lead to a great convenience for the following design of the firing logic because of the very same ACMs configuration in every virtual ring.

For most axial-symmetric aircrafts, the attitude control system usually consists of two parts. One is to control the angle of attack by elevator system, and the other is to control the angle of sideslip by rudder system, which are called longitudinal and latitudinal motion respectively. Similarly, the ACMs can be divided into longitudinal and latitudinal sections, and be used to improve the dynamic characteristics of pitch and yaw respectively. The divided sections are shown in Fig. 3.

In order to describe the state of the ACMs, the firing state array $N_{5\times 36}$ is defined here. The elements of this array can only be 1 or 0. $N(i,j)=0$ denotes the (i,j) motor has been used up and cannot be used again, while $N(i,j)=1$ denotes the (i,j) motor can be used. As indicated in the previous section, the forces generated by the ACMs cannot be changed continuously. Once it's fired, the thrust force will keep a constant for a fixed period. The distance between the center of the aircraft mass and every motor is denoted by l since the diameter of the ACMs can be ignored. Supposing F_f is the constant thrust that each motor generates in free fluid, the force and moment generated by the motor marked (i,j) can be described in the body-fixed frame of reference as

$$\begin{pmatrix}T_x\\T_y\\T_z\end{pmatrix} = \begin{pmatrix}0\\-K_f F_f\sin(2\pi(j-1)/36)\\-K_f F_f\cos(2\pi(j-1)/36)\end{pmatrix} \tag{6}$$

$$\begin{pmatrix}L_f\\M_f\\N_f\end{pmatrix} = \begin{pmatrix}0\\K_m F_f l\cos(2\pi(j-1)/36)\\-K_m F_f l\sin(2\pi(j-1)/36)\end{pmatrix} \tag{7}$$

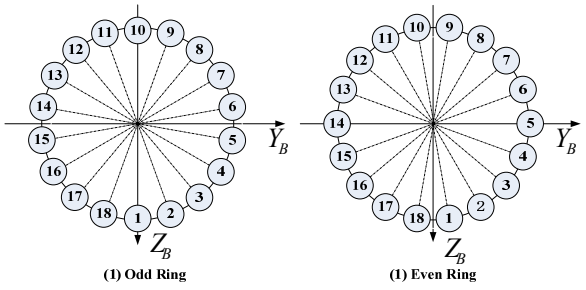

Figure 2. The configuration of the ACMs

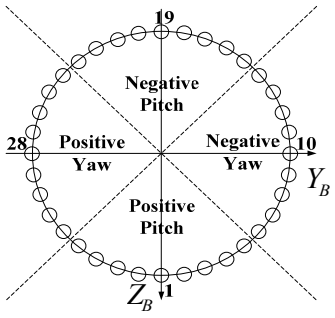

Figure 3. The virtual configuration of the ACMs

where K_f and K_m are the force and moment interaction amplification factors. Besides, because of the close location, there will be great mutual interference among the firing ACMs. Thus the number of the firing ACMs at the same time should be limited.

III. BLENDED CONTROL STRATEGY

When the future autonomous aircrafts (like PAC-3) are used to intercept airborne threats, "hit-to-kill" capability is required. At higher altitude or lower speed, this is an impossible task for the present-day aerodynamically controlled interceptors [9]. To maximize this probability, the RCS is applied to augment aerodynamic effectiveness and a blending logic to optimally allocate the RCS and aerodynamic fins should be employed. For the fuel of the RCS is limited, the aerodynamic fins are used for most of the flight phase as usual aircrafts, while the blended control strategy is operated only shortly before the intercept for terminal agility. In this paper, we focus on the homing phase during which the blended control strategy combining the aerodynamic fins and the RCS is designed. Since the attention is on the terminal of the guidance, we also assume the thrust generated by the main engine is zero.

This paper presents a blended control autopilot focusing on improving the speed of response. First, the controller of the aerodynamic subsystem is designed. Considering the dynamic response process of the state variables, the aerodynamic control subsystem can be divided into two loops by the theory of time-scale separation. The outer loop controller is for attitude angles, while the inner loop is for angular velocities. In each loop, the sliding mode control theory is also used to guarantee the robustness for the uncertainties. Besides, the aircraft in this paper is of skid-to-turn (STT), so the roll angle should be kept near zero. Then, the RCS is designed to improve the response speed. The RCS consists of four parts that are error dynamic adjustment model, PD controller, algorithm of firing logic and reaction jet model. The overall structure of the blended control system is shown in Fig. 4.

IV. AERODYNAMIC CONTROL SUBSYSTEM DESIGN

The design procedures of the aerodynamic controllers for the outer loop and the inner loop are almost the same. To reduce the length of the article, we only discuss the outer loop controller here.

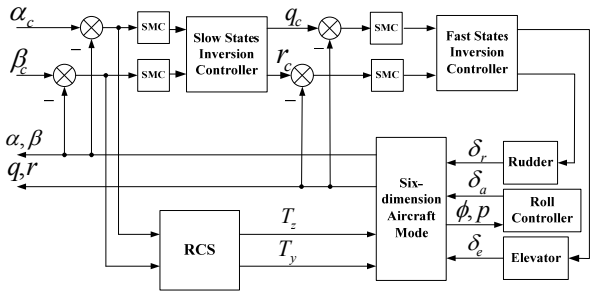

Figure 4. The blended control structure of the aircraft

A. Outer-loop feedback linearization controller

According to (1)-(2), the differential equations of the outer loop can be transformed into an affine nonlinear system as [10] [14]

$$\begin{pmatrix}\dot{\alpha}\\ \dot{\beta}\end{pmatrix}=\begin{pmatrix}f_{s1}\\ f_{s2}\end{pmatrix}+\begin{pmatrix}g_{s1}\\ g_{s2}\end{pmatrix}\begin{pmatrix}q\\ r\end{pmatrix} \tag{8}$$

where

$$\begin{aligned}f_{s1}&=-p\cos\alpha\tan\beta+QS\left[\cos\alpha C_{z0}-\sin\alpha C_x\right]/(mV\cos\beta)\\&\quad+Z_f\cos\alpha/(mV\cos\beta)\\ f_{s2}&=p\sin\alpha+(\cos\beta Y_f-\sin\alpha\sin\beta Z_f)/(mV)\\&\quad+QS\left[-\cos\alpha\sin\beta C_x+\cos\beta C_{y0}-\sin\alpha\sin\beta C_{z0}\right]/(mV)\\ g_{s1}&=\begin{bmatrix}1 & -\sin\alpha\tan\beta\end{bmatrix}\\ g_{s2}&=\begin{bmatrix}0 & -\cos\alpha\end{bmatrix}\end{aligned} \tag{9}$$

Obviously, the total relative degree of the system is 2. So the feedback linearization theory can be used to design the control law

$$u=\begin{pmatrix}q\\ r\end{pmatrix}=\begin{bmatrix}g_{s1}\\ g_{s2}\end{bmatrix}^{-1}\left[v-\begin{pmatrix}f_{s1}\\ f_{s2}\end{pmatrix}\right] \tag{10}$$

where v is called virtual control to be discussed in the next section. With u, the system is linearized and decoupled as

$$\begin{pmatrix}\dot{\alpha}\\ \dot{\beta}\end{pmatrix}=v \tag{11}$$

B. Outer-loop sliding mode controller [11]

The demanded attitude angles are recorded as (α_d, β_d), so the error of the angles can be written as

$$e_s=[\alpha_d-\alpha,\beta_d-\beta]^T \tag{12}$$

The sliding surface is defined as

$$s_s=c_s e_s+K_i\int e_s dt \tag{13}$$

where

$s_s=\begin{bmatrix}s_{s1} & s_{s2}\end{bmatrix}^T$, $c_s=diag\begin{bmatrix}c_{s1} & c_{s2}\end{bmatrix}$, $K_i=diag\begin{bmatrix}K_{i1} & K_{i2}\end{bmatrix}$.

An integrator $K_i\int e_s dt$ is adopted here to achieve zero steady state error in expected attitude angles.

Then an exponential approach rule is applied

$$\dot{s}_s = -\varepsilon_s \operatorname{sgn}(s_s) - k_s s_s \tag{14}$$

where

$$\varepsilon_s = diag\left[\varepsilon_{s1} \quad \varepsilon_{s2}\right], k_s = diag\left[k_{s1} \quad k_{s2}\right].$$

Following the above equations, we have

$$v = \begin{pmatrix} \dot{\alpha} \\ \dot{\beta} \end{pmatrix} = \begin{pmatrix} (\varepsilon_{s1} \operatorname{sgn}(s_{s1}) + k_{s1} s_{s1} + K_{i1} e_{s1}) / c_{s1} + \dot{\alpha}_d \\ (\varepsilon_{s2} \operatorname{sgn}(s_{s2}) + k_{s2} s_{s2} + K_{i2} e_{s2}) / c_{s2} + \dot{\beta}_d \end{pmatrix} \tag{15}$$

Substituting v into (10) yields the control

$$u = \begin{bmatrix} g_{s1} \\ g_{s2} \end{bmatrix}^{-1} \begin{bmatrix} (\varepsilon_{s1} \operatorname{sgn}(s_{s1}) + k_{s1} s_{s1} + K_{i1} e_{s1}) / c_{s1} + \dot{\alpha}_d - f_{s1} \\ (\varepsilon_{s2} \operatorname{sgn}(s_{s2}) + k_{s2} s_{s2} + K_{i2} e_{s2}) / c_{s2} + \dot{\beta}_d - f_{s2} \end{bmatrix} \tag{16}$$

In order to mitigate the influence of chattering, a saturation function $sat(s_s)$ is used to replace the signum function $\operatorname{sgn}(s_s)$ [16]

$$sat(s_s) = \begin{cases} 1 & s_s > \Delta \\ k s_s & |s_s| \le \Delta \quad k = 1/\Delta \\ -1 & s_s < -\Delta \end{cases} \tag{17}$$

where Δ is called the boundary layer.

C. Roll channel controller

The roll channel controller is used to keep the roll angle near zero. This research employs an outer roll angle loop with PID controller for steady state performance, and an inner roll rate loop for improving damping. The structure of the roll channel controller is shown in Fig. 5.

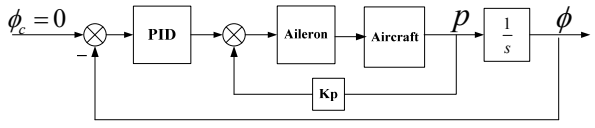

Figure 5. The structure of the roll channel controller

V. Reaction Jet Control Subsystem Design

A. Error dynamic adjustment model

Most of the blended control strategies are based on applying the aerodynamic subsystem to the utmost, and only operating the RCS when the former cannot offer sufficient control power. To compensate the insufficient force capability is the main idea in these strategies. However, the speed of maneuver response is much more important for the performance of intercepting [9][13]. So this research gives preferential treatment to the response speed of the control system. Once there exist large errors, it will increase the control instructions to the RCS, even if the aerodynamic subsystem can provide enough control power. Otherwise, it will decrease the control instructions to the RCS. An error dynamic adjustment model is used to achieve this.

This model consists of two nonlinear functions [17]:

$$\begin{cases} g(e) = (1 - |e|)^k \\ e_{RCS} = [1 - g(e)] \cdot e \end{cases} \tag{18}$$

where $k = 100$ here, $e(rad)$ is the error of the attitude angles, and $e_{RCS}(rad)$ is the dynamically adjusted control error. The angle of attack error and the sideslip angle error are to be adjusted respectively. Thus the control instructions to the RCS can be dynamically adjusted. A PD controller is designed after this model as the input instruction of the firing logic algorithm.

B. Firing logic algorithm

（1） The ACMs are of cyclic working with a firing cycle T and the nominal working time of each motor is denoted by τ. Choose $T = \tau = 20ms$ as shown in Fig. 6 [4].

（2） Control instructions are collected at every firing moment, then step (3) ~ (6) are operated. At other time the input instructions of the firing logic remain zero.

（3） The ACMs are fired only in the case of the demanded lateral thrust $P \ge P_0 (P_0 = 3000N)$.

（4） Before firing, the firing state array $N_{5\times36}$ should be checked to make sure which motors can be used. The firing sequence is arranged on the principle of generating the largest force. Thus the motors which are parallel to the symmetry axis in both longitudinal and latitudinal sections (Namely the motors with $j = 1$ or 19 in the longitudinal section and $j = 10$ or 28 in the latitudinal section) will be used firstly. The sequence of firing motors at the same placement of each ring is arranged on the principle of generating the largest moment. Thus the motors furthest to the aircraft's center of mass (Namely the motors with $i = 1$) will be used firstly.

（5） If the forces generated by the motors parallel to the symmetry axis are not sufficient, the motors which are the second closest to the symmetry axis will be fired symmetrically. The rest of the ACMs are all operated in this way.

（6） The firing state array $N_{5\times36}$ is updated after every firing cycle.

The structure of the RCS subsystem is shown in Fig. 7.

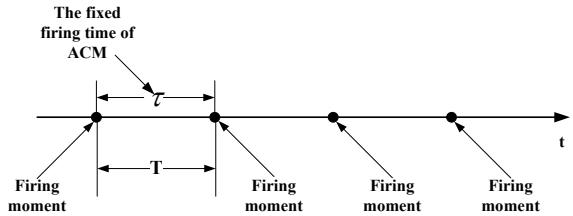

Figure 6. The working sequence of the ACMs [4]

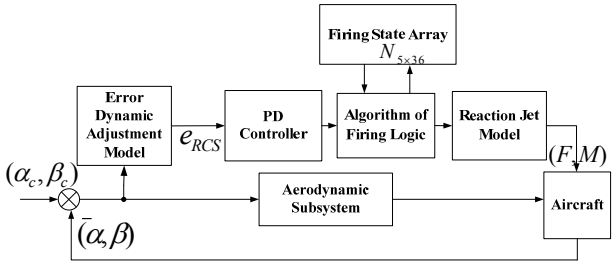

Figure 7. The structure of the RCS subsystem

VI. SIMULATION RESULTS

Simulations have been performed to verify the proposed blended control strategy. The initial flying parameters of the aircraft are chosen at an altitude $H=1000m$ and a speed $V=1200m/s$, with a trimmed angle of attack $\alpha_0=0.82\deg$ and angle of sideslip $\beta_0=0\deg$. The configuration data of the aircraft are from Ref. [3]. The fin actuators are assumed as a first order dynamics with a gain K. They all have a gain of 50, deflection limits of $\pm35\deg$ and rate limits of $\pm200\deg/s$. The nominal force generated by each ACM is assumed $F_f=3000N$, and the fixed working period is $20ms$.

Two kinds of uncertainties are applied in the simulation. One is the perturbation of aerodynamic coefficients with a range of $\pm20\%$. The other is the influence of interaction between aerodynamic flow and jet plumes which is indicated by the force and moment interaction amplification factors K_f and K_m. Since the accurate model of K_f and K_m cannot be obtained, random numbers uniformly distributed at the interval $[0.5,1.5]$ are used to represent them. The control instruction is $(\alpha_d,\beta_d)=(10^\circ,10^\circ)$, and the simulation results are shown in Fig. 8~11.

First, an ideal aircraft model is evaluated in Fig. 8 which illustrates the response curves of α,β,q,r using pure aerodynamic control and blended control respectively. Then the case with two kinds of uncertainties mentioned above is shown in Fig. 9. Fig. 8(a), (b) and Fig. 9(a), (b) indicate the achieved response characteristics of attitude angles relative to the command are dramatically improved with the blended control strategy, which is a great advantage for intercepting. Fig. 8(c), (d) and Fig. 9(c), (d) indicate the achieved angular velocities with the blended control strategy increase rapidly within a short time, and then decrease quickly. It further states the demanded attitude angles can be achieved early with the blended control strategy, since the area enclosed with the angular velocity curve and time axis is the magnitude of the attitude angle. Fig. 8 and Fig. 9 also show the blended control strategy has a strong robustness for uncertainties and disturbance.

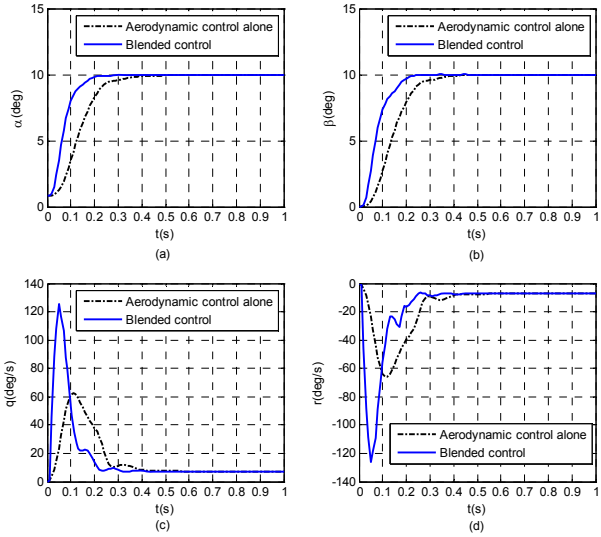

Figure 8. The response of α,β,q,r (ideal model)

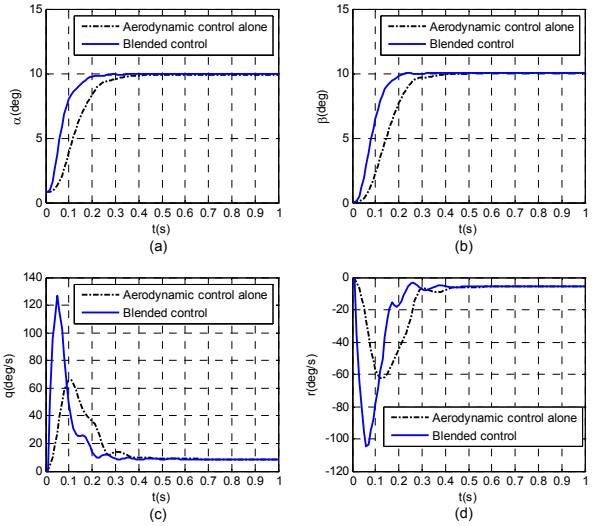

Figure 9. The response of α,β,q,r (model with uncertainties)

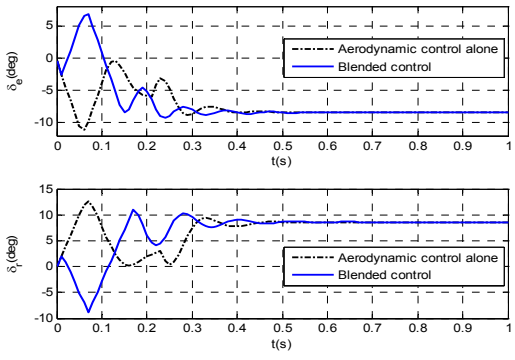

Figure 10. The deflections of the aerodynamic fins

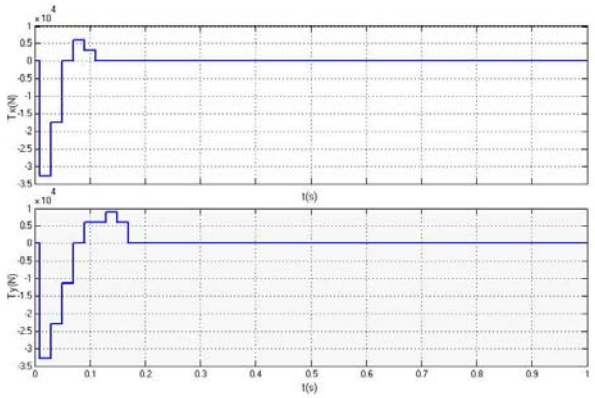

Figure 11. The lateral forces

The deflections of the aerodynamic fins are shown in Fig. 10. The figure shows a great performance in mitigating the influence of chattering, which is a major problem for the sliding mode control.

Fig. 11 shows the lateral forces in longitudinal and latitudinal directions respectively. It indicates the ACMs are fired only in the initial phase and the aerodynamic fins are used alone to maintain the desired command in the steady-state phase. Moreover, it shows that the ACMs are fired in one direction first to set up a large angular velocity in a very short time, and then those in the opposite direction are fired to decrease the angular velocity quickly. Besides, there is more than one firing cycle in setting up or diminishing the angular velocity, since the number of the firing ACMs at the same time is limited.

VII. CONCLUSION

This paper focuses on the homing phase of the guidance, and discusses the development of a blended control strategy using both aerodynamic fins and reaction jets. Feedback linearization based on the theory of time-scale separation and sliding mode control theory are applied to design the aerodynamic control subsystem, while an algorithm of firing logic which corresponds with the actual engineering characteristics of the ACMs is proposed. The blended control strategy is simulated in a nonlinear six-dimension aircraft model. Simulation results show the effectiveness of the blended control autopilot. With the new strategy, the response characteristic is dramatically improved and strong robustness for uncertainties and disturbance is also achieved.

REFERENCES

[1] A. Thukral, M. Innocenti, "A sliding mode missile pitch autopilot synthesis for high angle of attack maneuvering," *IEEE Transactions on Control System Technology*, Vol. 6, No. 3, May 1998, pp. 359-371.

[2] M. Innocenti, A. Thukral, "Simultaneous reaction jet and aerodynamic control of missile systems," *AIAA Guidance, Navigation and Control Conference*, Monterey, CA, Aug. 1993, pp. 347-354.

[3] C. Tournes, Y. Shtessel, I. Shkolnikov, "Autopilot for missiles steered by aerodynamic lift and divert thrusters using nonlinear dynamic sliding manifolds," *AIAA Guidance, Navigation and Control Conference and Exhibit*, San Francisco, California, Aug. 2005, AIAA-2005-6382.

[4] J. Wang , W. Chen, X. YIN, "Control policy design for missile using impulsive attitude control motors," *Systems Engineering and Electronics*, Vol. 30, No. 9, Sep. 2008, pp. 1724-1729.

[5] R. Herman, J. Butler, "Subsystems for the extended range interceptor (ERINT-1) missile," *AIAA SDIO Annual Interceptor Technology Conference*, Huntsville, AL, May 19-21, 1992, AIAA-92-2750.

[6] M. Xu, L. Liu, G. Tang, L. Zhu, "Research on attitude control of kinetic energy interceptor under blended operation of lateral thrust and aerodynamic force," *Journal of National University of Defense Technology,* Vol. 32, No. 4, Jan. 2010, pp. 30-36.

[7] P. K. Menon, V.R. Iragavarapu, "Adaptive techniques for multiple actuator blending," *AIAA Guidance, Navigation and Control Conference*, Boston, MA, Aug. 1998.

[8] P. K. Menon, E.J. Ohlmeyer, "Integrated design of agile missile guidance and autopilot systems," *Control Engineering Practice*, Vol. 9, No. 10, Oct. 2001, pp. 1095-1106.

[9] W. R. Chadwick, "Augmentation of high-altitude maneuver performance of a tail-controlled missile using lateral thrust," Naval Surface Warfare Center Dahlgren Division, May 1997.

[10] S. He, F Zhou, "Design of large angle attitude control system for agile missile," *Journal of System Simulation*, Vol. 23, No.5, May, 2011, pp. 906-910.

[11] C. Dong, F. Wang, X. Gao, Q. Wang, "Missile reaction-jet/aerodynamic compound control system design based on adaptive sliding mode control and fuzzy logic," *Acta Aeronautica et Astronautica Sinica*,Vol. 29, No1, Jan. 2008, pp. 165-169.

[12] R. Zhou, "Design of missile blended control system based on fuzzy logic," Contorl and Decision, Vol. 21, No. 7, Jul. 2006, pp. 825-828.

[13] L. Xing, K. Zhang, W. Chen, X. Yin, "Optimal control and output feedback considerations for missile with blended aero-fin and lateral impulsive thrust," *Chinese Journal of Aeronautics*, Vol. 23, No. 4, Jan. 2010, pp. 401-408.

[14] Y. Yao, Y. Bi, "Design of blended control strategy for missiles with lateral jets and aerodynamic surfaces," *Acta Aeronautica et Astronautica Sinica*, Vol. 31, No. 4, Apr. 2010, pp. 701-708.

[15] H. Zou, W. Chen, X. Yin, "Modeling and control of a spinning missile with blended aero-fin and lateral impulsive thrust," *Systems Engineering and Electronics*, Vol. 27, No. 4, Apr. 2005, pp. 687-691.

[16] H. K. Khalil, *Nonlinear Systems, 3rd ed.*, Prentice Hall, 2001, pp.557-558.

[17] G. Feng, "Controll allocation strategy for composite control of saucer-like air vehicle," *Journal of System Simulation*, Vol. 20, No. 4, Feb. 2008, pp.970-973.